metals

MDPI

Article

The Effect of Process Parameters on the Pore Structure of Lotus-Type Porous Copper Fabricated via Continuous Casting

Byung-Sue Shin and Soong-Keun Hyun *

Department of Materials Science and Engineering, Inha University, Incheon 22212, Republic of Korea; 22202189@inha.edu

* Correspondence: skhyun@inha.ac.kr; Tel.: +82-32-850-0215

Abstract: The pores in lotus-type porous copper are formed due to the difference in hydrogen solubility between the liquid and solid phases of copper. In a pressurized hydrogen atmosphere, hydrogen gas is released at the gas release and crystallization temperature, which is the melting point of copper. This study systematically analyzes the effects of process parameters, including hydrogen ratio, total pressure, and continuous casting speed, on the pore structure of lotus-type porous copper, with the aim of identifying the most critical process parameters for controlling pore diameter and density. Within the hydrogen ratio up to 50%, it was observed that as the hydrogen ratio increases, the pores tend to increase in porosity, and the pore diameter increases. As the hydrogen ratio increased from 25% to 50%, the pore diameter increased from 300 μm to 400 μm, while the pore density decreased from 3.3 $N{\cdot}mm^{-2}$ to 2.8 $N{\cdot}mm^{-2}$. As the total pressure increased, the pore diameter tended to decrease, and the pore density increased. Specifically, when the total pressure increased from 0.2 MPa to 0.4 MPa, the pore diameter decreased from 1100 μm to 400 μm, while the pore density increased significantly from 0.5 $N{\cdot}mm^{-2}$ to 2.8 $N{\cdot}mm^{-2}$. In addition, as the continuous casting speed increased, 30 to 90 $mm{\cdot}min^{-1}$, the pore diameter decreased from 850 μm to 400 μm, and the pore density increased from 0.7 $N{\cdot}mm^{-2}$ to 2.8. $N{\cdot}mm^{-2}$. Specifically, the increase in total pressure led to a decrease in Gibbs free energy and a reduction in the critical pore nucleation radius, which promoted pore formation and resulted in the creation of more, smaller pores. These results suggest that total pressure is the primary factor influencing both pore diameter and density in lotus-type porous copper.

Keywords: lotus-type porous copper; continuous casting; process parameter; porosity; pore diameter; pore density

Citation: Shin, B.-S.; Hyun, S.-K. The Effect of Process Parameters on the Pore Structure of Lotus-Type Porous Copper Fabricated via Continuous Casting. *Metals* **2024**, *14*, 1243. https://doi.org/10.3390/met14111243

Academic Editors: Hélder Puga, Heinz-Günter Brokmeier, Rongshan Qin and Oleg Mishin

Received: 14 October 2024
Revised: 28 October 2024
Accepted: 29 October 2024
Published: 31 October 2024

1. Introduction

Porous metals have low density and large specific surface areas, which allow them to be used in a wide range of applications, including lightweight materials, catalyst supports, electrodes, vibration and sound energy damping materials, and impact energy absorption materials [1,2]. While most porous metals have isotropic pore structures, lotus porous metals have an anisotropic pore structure characterized by long cylindrical pores aligned in one direction [2]. This anisotropy results from differences in scattering caused by dislocations and electrons, resulting in superior mechanical strength compared to conventional porous metals [3].

In particular, lotus-type porous copper has excellent thermal properties and a large specific surface area, making it a promising material for use in heat sinks [4–8]. It is also gaining attention as a cooling technology for next-generation electronic devices, such as electric vehicles (EVs), which use semiconductor devices with high heat generation densities. While conventional forced convection cooling systems require high power consumption, a novel cooling method that combines lotus-type porous copper with heat transfer surfaces significantly enhances the critical heat flux, providing an energy-efficient

cooling solution [9–11]. In addition, lotus-type porous copper has shown potential for application in heat pipes, providing high-efficiency heat exchange and energy-efficient cooling systems [12].

Recently, the miniaturization of semiconductor devices and the increase in current density have led to a significant increase in the heat generation density of power devices. For example, the heat generation density of SiC-based inverters for automotive applications is expected to reach 300–500 W/cm^2 [13]. This is significantly higher than that of conventional silicon (Si) power devices, requiring compact cooling solutions with high heat transfer performance. Lotus-type porous copper is proving to be an efficient material capable of satisfying these requirements [14].

The manufacturing of lotus-type porous metals is based on the principle that gases such as hydrogen, nitrogen or oxygen, which are insoluble in the solid phase, are soluble in the liquid phase [2,3,5,6]. As the molten metal solidifies, the difference in gas solubility between the liquid and solid phases leads to the formation of pores driven by insoluble gas atoms [2,14,15]. In this unidirectional solidification process, key parameters such as gas pressure, solidification rate, and melting temperature control the pore diameter, density, and porosity, allowing for the manufacturing of various porous metals.

The diameter, density, and shape of the pores in lotus-type porous copper are significantly influenced by the process parameters, especially the hydrogen ratio, total pressure, and continuous casting speed. The hydrogen ratio is a key factor in determining porosity and pore diameter, with higher hydrogen concentrations leading to an increase in both pore diameter and porosity [16]. In contrast, total pressure plays a critical role in decreasing pore diameter and increasing pore density [17]. As total pressure increases, gas expulsion is suppressed, resulting in smaller pores and higher pore density. Similarly, an increase in continuous casting speed accelerates the solidification process, resulting in the same effect: smaller pores and higher pore density [18].

Although there have been studies on the individual effects of process parameters on pore structure, comprehensive research that identifies which parameters are more effective and which parameters play a more critical role in controlling pore diameter and density is still lacking. Previous research [16–20] has primarily focused on analyzing the influence of individual process variables, such as the solidification rate or gas pressure, on pore formation, while in-depth analysis of the interactions between these process parameters has been relatively inadequate. As a result, the development of clear process strategies for achieving the optimal pore structure in lotus-type porous copper has been limited.

In this study, three key process parameters (hydrogen ratio, total pressure, and continuous casting speed) are systematically analyzed for their effects on the pore structure of lotus-type porous copper. The effects of each parameter on porosity, pore diameter, and density are evaluated to identify the critical factors that best control pore formation. In addition, the contributions of each parameter to the pore formation mechanism are evaluated to determine which has the greatest influence.

2. Materials and Methods

First, 2 kg of 99.99% pure copper was placed in a high-pressure chamber and evacuated using a rotary pump to create a vacuum. A mixed gas of hydrogen and nitrogen with hydrogen ratios of 25%, 34%, and 50% was pressurized between 0.2 and 0.4 MPa. The copper was melted by induction heating and held at 1628 K for 1800 s, with the temperature continuously monitored by an R-type thermocouple. To prevent premature flow of the molten copper, a start bar and a dummy bar were combined at the bottom of the crucible. The continuous casting process was initiated by lowering the start bar with a motor that controlled the continuous casting speed. The speed was adjustable between 1 and 100 $mm \cdot min^{-1}$, and for this study, casting speeds of 30, 60, and 90 $mm \cdot min^{-1}$ were used to control the solidification rate.

The hydrogen-saturated molten copper was cooled by a copper chiller as it moved to the lower chamber. During solidification, hydrogen was expelled at the solid–liquid

interface due to the significant difference in hydrogen solubility between the liquid and solid phases. Since the solubility of hydrogen in the liquid phase is much higher than in the solid phase, hydrogen gas formed cylindrical pores that grew parallel to the solidification direction. The resulting slab had a cross-section of 30 × 40 mm^2 and a length of 300–400 mm (Figure 1).

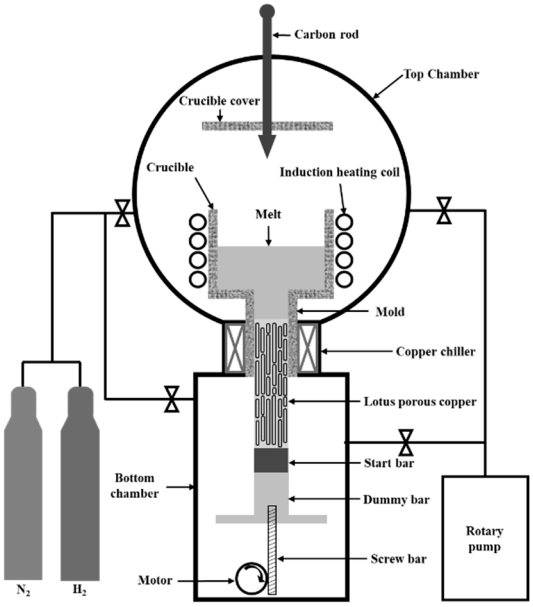

Figure 1. Schematic of the continuous casting apparatus.

The slab was cut both parallel and perpendicular to the casting direction using a wire-cut electric discharge machine (model AQ550L, Sodick Co., Yokohama, Japan). Each cross-section was polished with a series of sand papers and observed under an optical microscope (VHX-7000, Keyence Co., Osaka, Japan). Pore diameters and density were analyzed from the cross-section perpendicular to the casting direction using an image analyzer (Image-Pro Plus 6.1, Media Cybernetics Co., Silver Spring, MD, USA). Porosity was calculated from the weight and volume of the rectangular specimens.

3. Results

3.1. Hydrogen Ratio

The effects of various process parameters on the pore structure of lotus-type porous copper were analyzed by examining porosity, pore diameter, pore distribution, and pore density. The pore structure of lotus-type porous copper is mainly determined by the hydrogen solubility, pressure, and solidification rate [14]. In continuous casting, the hydrogen solubility is controlled by the hydrogen ratio, the pressure is controlled by a pressure chamber, and the solidification rate is controlled by adjusting the casting speed of the start bar. Therefore, the hydrogen ratio, total pressure, and continuous casting speed are the key process parameters in the continuous casting of lotus-type porous copper. Figure 2 shows the measured porosity results for different hydrogen ratios, with total pressure set at 0.4 MPa and continuous casting speed at 90 mm·min^{-1}. The results show a trend of increasing porosity from 36% to 53% as the hydrogen ratio increased from 25% to 50%.

Figure 3 shows the changes in pore morphology as a function of hydrogen ratio under the same conditions as in Figure 2, with a total pressure of 0.4 MPa and a continuous casting speed of 90 mm·min^{-1}. An analysis of the pore shape in both the perpendicular and parallel directions to the continuous casting direction showed a tendency for the pore diameter to increase with increasing hydrogen ratio.

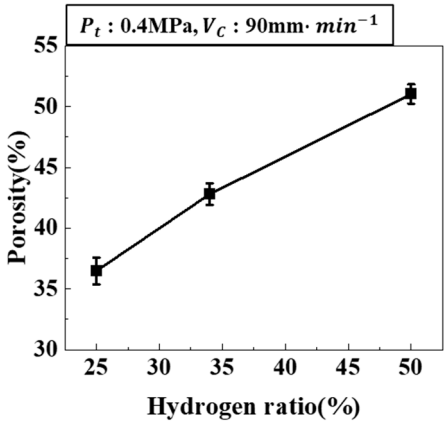

Figure 2. Porosity as a function of hydrogen ratio at a total pressure of 0.4 MPa, with a continuous casting speed of 90 mm·min^{-1}.

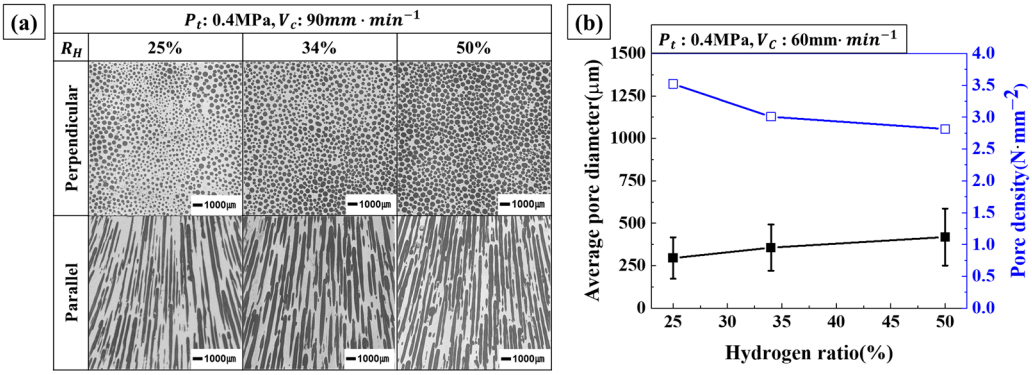

Figure 3. Pore morphology and diameter as a function of hydrogen ratio at a total pressure of 0.4 MPa and a continuous casting speed of 90 mm·min^{-1}: (**a**) cross-section perpendicular and parallel to the casting direction, and (**b**) measured pore diameter and pore density.

As shown in Figure 3b, the average pore diameter tended to increase from 300 μm to 400 μm with the hydrogen ratio increasing from 25% to 50%. There was a trend of increasing variation in pore diameter with higher hydrogen ratios because the pressurized hydrogen atmosphere in continuous casting dissolves hydrogen in the molten copper, leading to pore formation during solidification. In contrast, the pore density tended to decrease from 3.3 N·mm^{-2} to 2.8 N·mm^{-2} as the hydrogen ratio increased. According to Sieverts' Law, the hydrogen concentration is proportional to the square root of the hydrogen pressure. Conversely, according to Boyle's Law, the gas volume in the pores is inversely proportional to the external gas pressure, since the pore pressure equals the external gas pressure. Therefore, the increase in porosity and pore diameter with an increasing hydrogen ratio is primarily due to the greater influence of hydrogen solubility [2,16].

3.2. Total Pressure

Figure 4 shows the changes in porosity as a function of total pressure when the hydrogen ratio is 50% in a hydrogen–nitrogen mixed gas, and the continuous casting speed is set at 90 mm·min^{-1}. The experimental results confirmed a trend of decreasing porosity from 53% to 47% as the total pressure increased from 0.2 MPa to 0.4 MPa. This decrease in porosity is attributed to the suppression of pore formation as the total pressure increases.

Figure 5 shows the pore morphology in both parallel and perpendicular directions as the total pressure increases while the hydrogen ratio and continuous casting speed remain constant. The experimental results indicate that the pore diameter tends to decrease as the total pressure increases, while the number of observed pores increases. In particular, a larger distribution of smaller pores was observed.

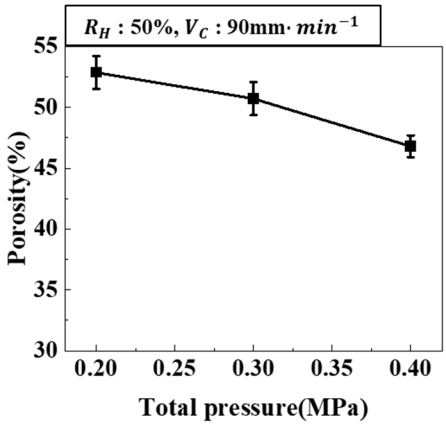

Figure 4. Porosity as a function of total pressure at a hydrogen ratio of 50%, with a continuous casting speed of 90 mm·min^{-1}.

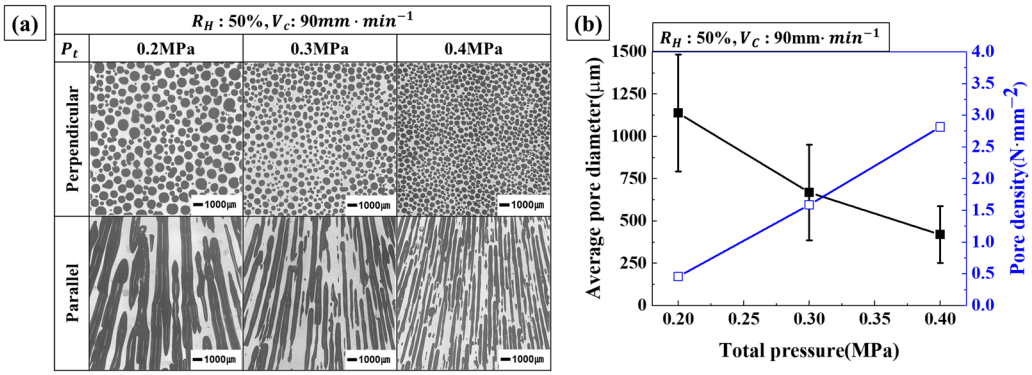

Figure 5. Pore morphology and diameter as a function of total pressure at a hydrogen ratio of 50% and a continuous casting speed of 90 mm·min^{-1}: (**a**) cross-section perpendicular and parallel to the casting direction, and (**b**) measured pore diameter and pore density.

Figure 5b shows the changes in pore diameter and pore density with increasing total pressure. The measurements show that as the total pressure increases from 0.2 MPa to 0.4 MPa, the pore diameter tends to decrease from 1100 μm to 400 μm, while the pore density increases sharply from 0.5 N·mm^{-2} to 2.8 N·mm^{-2}. Therefore, as the total pressure increases, both porosity and pore diameter decrease, but the total number of pores increases due to the increase in pore density.

3.3. Continuous Casting Speed

The continuous casting speed is closely related to the solidification rate, with the solidification rate increasing as the continuous casting speed increases. Figure 6 shows the changes in porosity as a function of continuous casting speed when the hydrogen ratio and total pressure are kept constant. The experimental results show that the average porosity remained unchanged at 52% as the continuous casting speed increased from 30 to 90 mm·min^{-1}. Therefore, it was found that changes in continuous casting speed had little to no effect on porosity.

Figure 7a shows the pore morphology as a function of increasing continuous casting speed while keeping the hydrogen ratio and total pressure constant. As the continuous casting speed increased 30 to 90 mm·min^{-1}, the pore diameter decreased, while the number of pores observed increased. In addition, a larger distribution of smaller pores was observed.

Figure 7b shows the measured pore diameter and pore density as a function of increasing continuous casting speed. As the continuous casting speed increased from 30 to 90 mm·min^{-1}, the average pore diameter decreased from 850 μm to 400 μm, while the pore density increased sharply from 0.7 N·mm^{-2} to 2.8 N·mm^{-2}. Therefore, as the continuous

casting speed increases, the porosity remains constant, the pore diameter decreases, but the pore density increases, resulting in an overall increase in the number of pores.

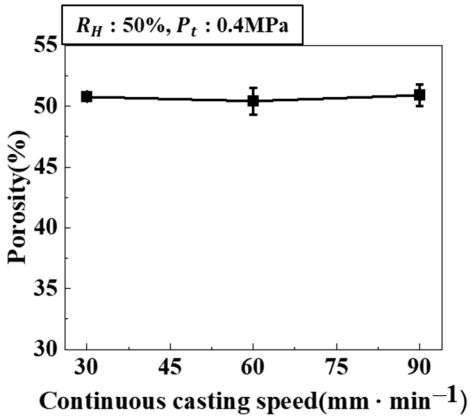

Figure 6. Porosity as a function of continuous casting speed at a hydrogen ratio of 50%, with a total pressure of 0.4 MPa.

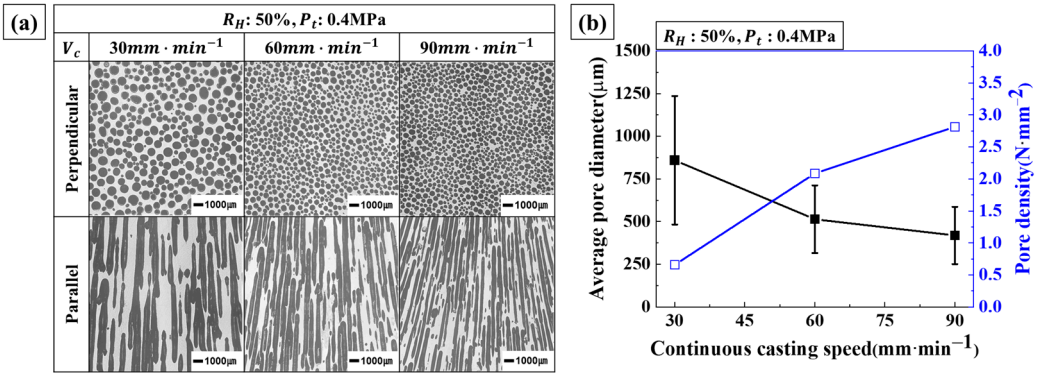

Figure 7. Pore morphology and diameter as a function of continuous casting speed at a hydrogen ratio of 50% and total pressure of 0.4 MPa: (**a**) cross-section perpendicular and parallel to the casting direction, and (**b**) measured pore diameter and pore density.

4. Discussion

4.1. Porosity

Pore formation in lotus-type porous copper occurs due to the difference in hydrogen solubility between liquid and solid copper. The porosity varies depending on the amount of hydrogen gas expelled during the solidification process as the copper transitions from a hydrogen-saturated liquid state to a solid state with lower hydrogen solubility [16,21–23]. In the copper–hydrogen system, hydrogen solubility can be calculated based on temperature and phase (liquid or solid) using Sieverts' Law, where the hydrogen concentration is proportional to the square root of hydrogen pressure and temperature [2,14].

The amount of rejected hydrogen is determined by the difference in solubility between the liquid and solid phases of copper. Therefore, porosity can be estimated by calculating the volume ratio of hydrogen rejected during gas evolution crystallization in a hydrogen atmosphere to the volume of pores formed [2,16,21]. Porosity is expressed in terms of pore volume (V_ρ) and solid copper volume (V_S) as shown in Equation (1) [18,21].

$$\varepsilon \approx \frac{V_\rho}{V_\rho + V_S} \cdot 100 \quad (1)$$

where ε represents the porosity. Since the pore volume varies with the amount of rejected hydrogen, the pore volume is described using Equation (2) as follows [18]:

$$V_\rho = \frac{(k_l - k_s)\sqrt{P_{H_2}} \cdot R \cdot T_m}{P_{N_2} + P_{H_2}} \quad (2)$$

$$\varepsilon \approx \frac{(k_l - k_s) \cdot R \cdot T_m}{(k_l - k_s) \cdot R \cdot T_m + m \cdot V_s \cdot \frac{P_{N_2} + P_{H_2}}{\sqrt{P_{H_2}}}} \quad (3)$$

P_{N_2} is the partial pressure of nitrogen and P_{H_2} is the partial pressure of hydrogen. R is the gas constant, and Tm is the crystallization temperature at which the rejected hydrogen gas is released, which is the melting point of copper. k_l is the equilibrium constant for the hydrogen solubility reaction in liquid copper, and k_s is the equilibrium constant for the hydrogen solubility reaction in solid copper. m is a fitting parameter that accounts for the amount of escaping hydrogen [14,16,18]. As shown in Equations (2) and (3), the porosity is determined by the total pressure and the partial pressure of hydrogen. Therefore, the continuous casting speed has little effect on porosity, and as shown in the results of Figure 6, changes in continuous casting speed result in minimal changes in porosity.

As the hydrogen ratio increases, the porosity increases because, as described by Equation (3), the pore volume increases in proportion to the square root of the hydrogen partial pressure, leading to an increase in porosity [16]. Since nitrogen does not dissolve in molten copper, the pores are composed entirely of hydrogen. In addition, the pore pressure must balance the total pressure, so if the total pressure is constant, the pore pressure remains stable regardless of changes in the hydrogen partial pressure. As a result, an increase in the hydrogen ratio increases the solubility of hydrogen in the molten copper, which ultimately leads to an increase in porosity at constant total pressure [2,14,16]. On the other hand, as the total pressure increases, the pore volume decreases, resulting in a decrease in porosity. In other words, higher total pressure makes it more difficult for gas to diffuse into the pores, which, in turn, reduces the partial pressure of hydrogen required for pore formation, resulting in a decrease in porosity [22,24].

4.2. Pore Diameter

In lotus-type porous copper, pore nucleation occurs due to the difference in hydrogen solubility between liquid and solid copper. The hydrogen dissolved in the liquid copper is expelled as the copper crystallizes into a solid phase, as it cannot enter the solid copper. This expulsion creates pores that eventually form pores [22].

The nucleation of pores based on the hydrogen ratio is related to the nucleation rate J and the Gibbs free energy. The relationship between the nucleation rate J and the Gibbs free energy of a pore is given by [18,25]:

$$J = \frac{NkT}{h} exp\left(-\frac{1}{kT} \cdot \frac{16\pi}{3} \cdot \frac{\gamma^3}{\Delta P^2} \cdot f(\theta)\right) \quad (4)$$

where N is the number of gas molecules in the liquid phase, k is the Boltzmann constant, T is the temperature, h is Planck's constant, γ is the surface energy of the pores, ΔP is the difference between the ambient pressure and the internal pressure of the pores, and (θ) is a function of the surface energy, which depends on the contact angle θ between the solid and the pores. The nucleation rate based on the hydrogen ratio is related to N, where the hydrogen concentration in the liquid phase increases as the hydrogen ratio increases. This leads to a proportional increase in the number of hydrogen molecules in the liquid, which means that the hydrogen ratio and N are directly proportional.

As the hydrogen ratio increases at a constant total pressure, the hydrogen concentration in the pores increases, promoting pore growth. The diffusion of hydrogen into the pores increases the internal pore pressure, resulting in an increase in pore diameter [16,22,24]. Consequently, as the hydrogen ratio increases, the pore diameter tends to increase. In addition, the increase in hydrogen partial pressure increases porosity, which, in turn, promotes pore nucleation. The nucleated pores move closer together and overlap, resulting in larger pore

diameter and a decrease in pore density [15]. The relationship between total pressure, continuous casting speed, and pore diameter is explained as follows. Pores form through heterogeneous nucleation [2,14,16–20], with changes in Gibbs free energy ($\Delta G'_{het}$) and the critical pore nucleation radius (r'_{het}) during pore formation described by Equations (4)–(6) [17,26].

$$\Delta G = \Delta G_i + \Delta G_v = 4\pi r^2 \cdot \sigma_{L-G} - \frac{4}{3}\pi r^3 \cdot P_i \tag{5}$$

$$\Delta G'_{het} = \Delta G \cdot f(\theta, \Gamma) = \frac{1}{9} \cdot \Delta G_i(r'_{het}) \cdot f(\theta, \Gamma) \tag{6}$$

$$r'_{het} = \frac{2\sigma_{L-G}}{3\left(P_{vap} + P_{H_2} + P_{N_2} + \sigma_L g h\right)} \tag{7}$$

In heterogeneous nucleation of these pores, for a cone with an angle Γ and depth h, the shape factor $f(\theta, \Gamma)$ is calculated based on the interfacial tension balance [17].

$$\sigma_{G-S} = \sigma_{L-S} - \sigma_{L-G} \cdot \cos\theta \tag{8}$$

$$f(\theta, \Gamma) = \frac{[1 - \sin\left(\theta + \frac{\Gamma}{2}\right)]}{4 \cdot \sin\left(\frac{\Gamma}{2}\right)} \cdot \left\{2\sin\left(\frac{\Gamma}{2}\right) - \cos\theta\left[1 + \sin\left(\theta + \frac{\Gamma}{2}\right)\right]\right\} \tag{9}$$

where ΔG_i is the driving force for pore formation, which represents the effect of pore movement per unit volume of the melt, ΔG_v is the resistance to pore nucleation, resulting from the increase in surface free energy. σ_{L-G} is the surface tension between the liquid and gas phases, and P_i is the internal pressure of the pore, which can be calculated as follows [17,20].

$$P_i = P_{vap} + P_{H_2} + P_{N_2} + \sigma_L g h + \frac{2\sigma_{L-G}}{r} \tag{10}$$

According to Equations (5)–(9), the changes in Gibbs free energy and critical pore nucleation radius associated with the heterogeneous nucleation of pores were calculated as a function of total applied pressure, and the results are shown in Figure 8. The variables used in the calculations are listed in Table 1. It was observed that as the total pressure increases, both the Gibbs free energy and the critical pore nucleation radius decrease. Therefore, heterogeneous pore nucleation becomes easier as the total pressure increases. In addition, the pressure difference between the inside and outside of the pores increases as the total pressure increases, leading to an increase in the pore nucleation rate [27]. This suggests that as the Gibbs free energy and critical pore nucleation radius decrease, pore nucleation is promoted, resulting in an increase in the number of pores and a decrease in the pore diameter.

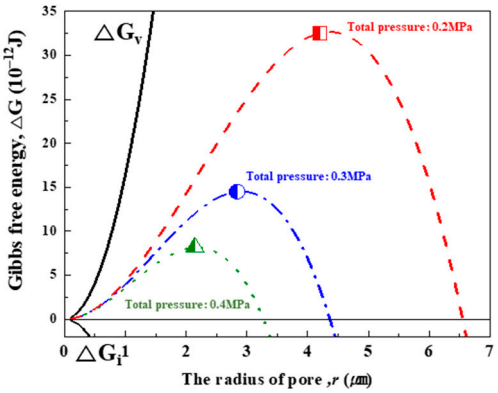

Figure 8. Variations in Gibbs free energy and critical pore nucleation radius are influenced by total pressure, with hydrogen gas release and crystallization temperature set at the melting point of copper at 1080 °C.

Table 1. Variables for the calculation of Gibbs free energy and critical pore nucleation radius in pore nucleation (Reprinted from ref. [17]).

Metal	$\sigma_L gh$, Pa	P_{vap}, Pa	θ, °	σ_{L-G}, J·m^{-2}
Cu	7840	1.28	134	1.31

Figure 9a–c show the measured results of the solid–liquid interface shape angle as a function of continuous casting speed. Since the pores in lotus-type porous copper grow perpendicular to the solid–liquid interface [18], the angle of the pores was measured based on the continuous casting speed, and the cone angle of the solid–liquid interface was analyzed. Because pore growth takes place in the perpendicular direction, variations in the continuous casting speed also lead to variations in the shape angle of the solid–liquid interface. Figure 9d shows the shape angle as a function of distance from the sample center based on the continuous casting speed. The experimental results indicate that as the continuous casting speed increases, the cone angle of the solid–liquid interface tends to decrease. These variations in angle directly affect the directionality and growth mechanism of pore formation at the solid–liquid interface. Based on the measured angle values, the variations in Gibbs free energy ($\Delta G'_{het}$) associated with heterogeneous nucleation were calculated, and the results are shown in Figure 10.

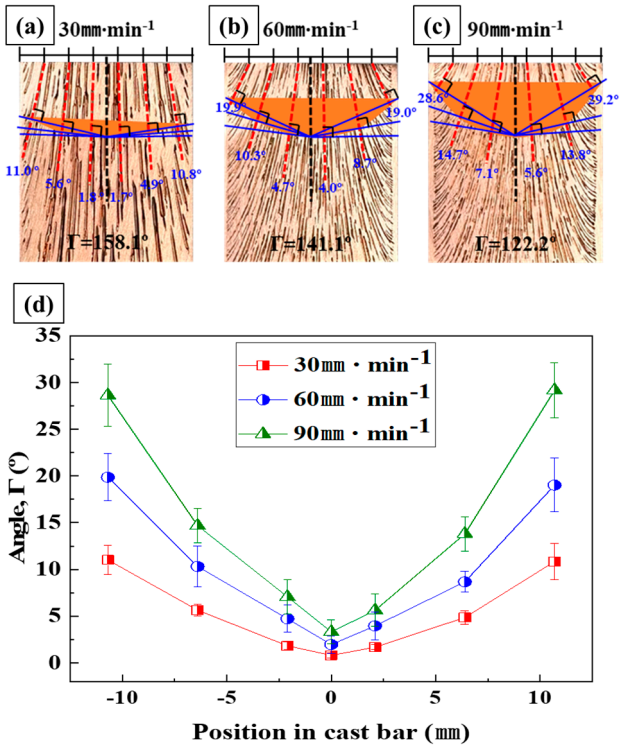

Figure 9. The measured angle of pores between the direction of pore growth and the direction of transfer in the cross section of the ingot as a continuous casting speed (**a**) 30 mm·min^{-1}; (**b**) 60 mm·min^{-1}; (**c**) 90 mm·min^{-1}; (**d**) measured angle between the pore and the solid–liquid interface.

Figure 10a shows that as the continuous casting speed increases, the angle of the solid–liquid interface decreases, leading to a decrease in the shape factor f(θ, Γ). The shape factor is an important parameter in the heterogeneous nucleation of pores, and a decrease in the angle indicates that the energy barrier required for pore formation is lowered. Based on these changes, the calculated variations in the Gibbs free energy can be observed in Figure 10b–d.

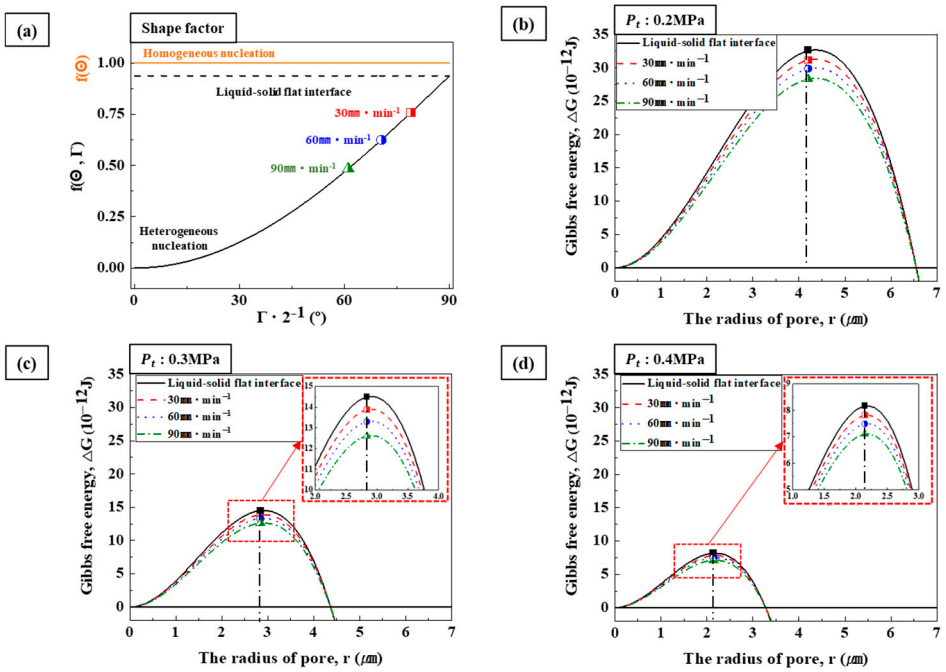

Figure 10. Variations in Gibbs free energy and critical pore nucleation radius with changes of total pressure. (**a**) Shape factor calculated by Equation (9) as a continuous casting speed, (**b**) total pressure 0.2 MPa, (**c**) total pressure 0.3 MPa, (**d**) total pressure 0.4 MPa.

As the continuous casting speed increases, the critical pore nucleation radius remains constant, while the change in Gibbs free energy tends to gradually decrease. This indicates that as the continuous casting speed increases, the energy barrier for pore formation is lowered, making heterogeneous nucleation of pores easier [2,17,18]. Therefore, as the continuous casting speed increases, the Gibbs free energy during pore nucleation tends to decrease, resulting in an increase in the number of pores and a decrease in the pore diameter.

By comparing Figures 9 and 10, it can be observed that the changes in Gibbs free energy and critical pore nucleation radius decrease significantly as the total pressure increases. Conversely, while the Gibbs free energy change decreases with continuous casting speed, the critical nucleation radius remains constant.

By comparing the results for pore diameter and density in Figures 5 and 7 as a function of total pressure and continuous casting speed, it can be seen that pore density increases consistently with both parameters. However, higher total pressure results in a more significant decrease in pore diameter along with an increase in pore density. This phenomenon is attributed to the decrease in Gibbs free energy change and critical pore nucleation radius during heterogeneous nucleation of pores with increasing total pressure.

In addition, while the cone angle of the solid–liquid interface decreases with an increase in continuous casting speed, the Gibbs free energy associated with heterogeneous nucleation decreases only slightly and does not affect the critical pore nucleation radius. Therefore, it can be concluded that the total pressure is the key process parameter that significantly affects the pore density and size in the manufacturing of lotus-type porous copper by continuous casting.

5. Conclusions

In this study, the effects of process parameters, such as hydrogen ratio, total pressure, and continuous casting speed, on the pore structure during the manufacturing of lotus-type porous copper were analyzed. Based on the results, the following conclusions can be made:

1. Hydrogen ratio: As the hydrogen ratio increases from 25% to 50%, the porosity tends to increase due to the higher solubility of hydrogen in the molten copper as the

hydrogen partial pressure increases. In contrast, an increase in total pressure inhibits pore formation, resulting in a decrease in porosity. The continuous casting speed has a minimal effect on porosity, indicating that the hydrogen ratio and total pressure are the primary factors determining porosity. Also, for the pore diameter and density, as the hydrogen ratio increases, the pore diameter tends to increase, while the pore density decreases. The diffusion of hydrogen into the pores increases the internal pore pressure, resulting in an increase in pore diameter. The increase in hydrogen partial pressure increases porosity and promotes pore nucleation. The nucleated pores move closer together and overlap, resulting in larger pore diameters and a decrease in pore density.

2. Total pressure: As the total pressure increases, the pore diameter tends to decrease while the pore density increases sharply. This is due to the decrease in Gibbs free energy with increasing total pressure, which leads to a smaller critical pore nucleation radius. As smaller pores are generated more frequently, the total pore diameter decreases and the pore density increases. In particular, as the total pressure increases from 0.2 MPa to 0.4 MPa, a significant reduction in pore diameter is observed from 1100 μm to 400 μm, along with a rapid increase in pore density from 0.5 $N \cdot mm^{-2}$ to 2.8 $N \cdot mm^{-2}$. This demonstrates the critical role that total pressure plays in changing the pore structure.
3. Continuous casting speed: The effect of continuous casting speed on pore diameter and density was also observed. As the casting speed increases from 30 to 90 $mm \cdot min^{-1}$, the solidification rate accelerates, causing the pore diameter to decrease from 850 μm to 400 μm, while the pore density increases from 0.7 to 2.8 $N \cdot mm^{-2}$. This occurs because faster solidification reduces the time available for hydrogen to escape from the pores, resulting in smaller pore sizes and a larger number of smaller pores. In particular, as the continuous casting speed increases, the cone angle of the solid–liquid interface decreases, facilitating heterogeneous nucleation of pores and contributing to the increase in pore density.
4. Both total pressure and continuous casting speed contribute to the increase in pore density; however, this study shows that total pressure has a significantly greater effect on both the pore diameter and density. Therefore, controlling the total pressure is the most critical factor for effectively controlling the pore structure of lotus-type porous copper.

Author Contributions: Conceptualization, B.-S.S.; methodology, B.-S.S.; software, B.-S.S.; validation, S.-K.H.; formal analysis, S.-K.H.; investigation, B.-S.S.; writing—review and editing, S.-K.H.; supervision, S.-K.H. All authors have read and agreed to the published version of the manuscript.

Funding: This work was supported by INHA UNIVERSITY Research Grant.

Data Availability Statement: The raw data supporting the conclusions of this article will be made available by the authors on request.

Conflicts of Interest: The authors declare no conflicts of interest.

References

1. Banhart, J. Manufacture, Characterization and Application of Cellular Metals and Metal Foams. *Prog. Mater. Sci.* **2001**, *46*, 559–632. [CrossRef]
2. Nakajima, H. Fabrication, properties and application of porous metals with directional pores. *Prog. Mater. Sci.* **2007**, *52*, 1091–1173. [CrossRef]
3. Hyun, S.K.; Ikeda, T.; Nakajima, H. Fabrication of lotus-type porous iron and its mechanical properties. *Sci. Technol. Adv. Mater.* **2004**, *5*, 201–205. [CrossRef]
4. Fink, M.; Andersen, O.; Seidel, T.; Schlott, A. Strongly orthotropic open cell porous metal structures for heat transfer applications. *Metals* **2018**, *8*, 554. [CrossRef]
5. Ogushi, T.; Chiba, H.; Nakajima, H. Development of lotus-type porous copper heat sink. *Mater. Trans.* **2006**, *47*, 2240–2247. [CrossRef]

6. Liu, X.; Li, Y.; Zhang, H.; Liu, Y.; Chen, X. Effect of pore structure on heat transfer performance of lotus-type porous copper heat sink. *Int. J. Heat Mass Transf.* **2019**, *144*, 118641. [CrossRef]
7. Zhang, H.; Chen, L.; Liu, Y.; Li, Y. Experimental study on heat transfer performance of lotus-type porous copper heat sink. *Int. J. Heat Mass Transf.* **2013**, *56*, 172–180. [CrossRef]
8. Chiba, H.; Ogushi, T.; Nakajima, H. Heat transfer capacity of lotus-type porous copper heat sink for air cooling. *J. Therm. Sci. Technol.* **2010**, *5*, 222–237. [CrossRef]
9. Kibushi, R.; Yuki, K.; Unno, N.; Ogushi, T.; Murakami, M.; Numata, T.; Ide, T.; Nomura, H. Enhancement of the critical heat flux of saturated pool boiling by the breathing phenomenon induced by lotus copper in combination with a grooved heat transfer surface. *Int. J. Heat Mass Transf.* **2021**, *179*, 121663. [CrossRef]
10. Terada, M.; Yuki, K.; Unno, N.; Kibushi, R.; Ogushi, T.; Murakami, M.T.; Numata, T.I.; Nomura, H. Heat transfer performance of two-phase immersion cooling by breathing phenomena with different pore structures of lotus copper. In Proceedings of the 2022 International Conference on Electronics Packaging (ICEP), Sapporo, Japan, 11–14 May 2022; pp. 103–104. [CrossRef]
11. Thangavel, P.; Sekar, A. Investigations on heat transfer characteristics of porous type copper heat sink with bifurcations. *J. Therm. Eng.* **2021**, *7*, 584–594. [CrossRef]
12. Supriadi, S.; Putra, N.; Ariantara, B.; Indhiarto, I. Fabrication of a lotus-type porous material to be applied in heat pipe wick. *Evergreen* **2021**, *8*, 855–860. [CrossRef]
13. Ogushi, T.; Ide, T. Thermal Solution for Cooling of Electronic Equipment using Lotus-type Porous Copper Heat Sink. In Proceedings of the 2021 Third International Symposium on 3D Power Electronics Integration and Manufacturing (3D-PEIM), Osaka, Japan, 21–23 June 2021; pp. 1–6. [CrossRef]
14. Nakajima, H. Fabrication, mechanical and physical properties, and its application of lotus-type porous metals. *Mater. Trans.* **2019**, *60*, 2481–2489. [CrossRef]
15. Shapovalov, V.I. Formation of ordered gas-solid structures via solidification in metal-hydrogen systems. *MRS Online Proc. Libr. (OPL)* **1998**, *521*, 281. [CrossRef]
16. Yamamura, S.; Shiota, H.; Murakami, K.; Nakajima, H. Evaluation of porosity in porous copper fabricated by unidirectional solidification under pressurized hydrogen. *Mater. Sci. Eng. A* **2001**, *318*, 137–143. [CrossRef]
17. Song, Q.L.; Jin, Q.L.; Li, Z.J.; Zhou, R. Effects of pore nucleation, growth and solidification mode on pore structure and distribution of lotus type porous copper. *Trans. Indian Inst. Met.* **2017**, *70*, 1437–1445. [CrossRef]
18. Park, J.S.; Hyun, S.K.; Suzuki, S.; Nakajima, H. Effect of transference velocity and hydrogen pressure on porosity and pore morphology of lotus-type porous copper fabricated by a continuous casting technique. *Acta Mater.* **2007**, *55*, 5646–5654. [CrossRef]
19. Liu, X.; Li, X.; Jiang, Y.; Xie, J. Effect of casting temperature on porous structure of lotus-type porous copper. *Procedia Eng.* **2012**, *27*, 490–501. [CrossRef]
20. LIU, Y.; Zhang, H.W.; Li, Y.X. Effect of melt superheat on structural uniformity of lotus-type porous metals prepared by unidirectional solidification. *Trans. Nonferrous Met. Soc. China* **2015**, *25*, 1004–1010. [CrossRef]
21. Nakahata, T.; Nakajima, H. Fabrication of lotus-type porous silicon by unidirectional solidification in hydrogen. *Mater. Sci. Eng. A* **2004**, *384*, 373–376. [CrossRef]
22. Lee, P.D.; Atwood, R.C.; Dashwood, R.J.; Nagaumi, H. Modeling of porosity formation in direct chill cast aluminum–magnesium alloys. *Mater. Sci. Eng. A* **2002**, *328*, 213–222. [CrossRef]
23. Campbell, J. *Castings Practice: The Ten Rules of Castings*; Elsevier: Amsterdam, The Netherlands, 2004; pp. 108–113.
24. Wei, P.S.; Luo, C.W.; Hsieh, I.C. Scaling of inter-pore spacing of lotus-type pores. *Phys. Scr.* **2023**, *98*, 085943. [CrossRef]
25. Fisher, J.C. The fracture of liquids. *J. Appl. Phys.* **1948**, *19*, 1062. [CrossRef]
26. Hirth, J.P. *Progress in Materials Science: Condensation and Evaporation*; Pergamon Press: Oxford, UK, 1963; Volume 11.
27. Drenchev, L.; Sobczak, J.; Malinov, S.; Sha, W. Gasars: A class of metallic materials with ordered porosity. *Mater. Sci. Technol.* **2006**, *22*, 1135–1147. [CrossRef]